The Anti-Apoptotic Protein PEA-15 Is a Tight Binding Inhibitor of ERK1 and ERK2, Which Blocks Docking Interactions at the D-Recruitment Site†

Kari Callaway,‡ Olga Abramczyk,§ Lance Martin,|| and Kevin N. Dalby*,‡,§,⊥

Division of Medicinal Chemistry, University of Texas at Austin, Texas 78712, Graduate Programs in Biochemistry and Molecular Biology, University of Texas at Austin, Texas 78712, and Department of Biochemistry, Stanford University, Stanford, California 94305

Received January 31, 2007; Revised Manuscript Received June 4, 2007

ABSTRACT: PEA-15 is a small anti-apoptotic protein that is enriched in astrocytes, but expressed in a broad range of tissues. It sequesters the protein kinases ERK1 and 2 in the cytoplasm, thereby limiting their proximity to nuclear substrates. Using a fluorescence anisotropy approach, PEA-15 is shown to be a high-affinity ligand for both ERK1 and 2, exhibiting a dissociation constant in the range of $K_d = 0.2-0.4$ μM, regardless of their activation states. Neither the phosphorylation of PEA-15 (phospho Ser-104 and/or phospho Ser-116) nor the phosphorylation of ERK1/2 (by MKK1) significantly affects the stability of the ERK/PEA-15 interaction, and therefore it does not directly regulate the release of ERK2 to the nucleus. The extreme C-terminus of PEA-15 was previously shown by mutagenesis to be important for ERK2 binding; however, the site of binding was not established. Here it is demonstrated that the D-recruitment site (DRS) of ERK2 binds PEA-15, probably at the C-terminus, and renders PEA-15 an inhibitor of ERK2 docking interactions. Using fluorescence anisotropy competition assays it is shown that PEA-15 competes for binding to ERK1/2 with a peptide derived from the D-site of Elk-1, which binds the DRS of ERK1/2. Using modified ERK2 proteins containing single cysteine residues, PEA-15 was shown to protect single cysteines situated within the DRS from alkylation. The pattern and magnitude of protection were very similar to those induced by the binding of the peptide derived from the D-site of Elk-1. These and published data support the notion that PEA-15 binds two sites on ERK1/2 in a bidentate manner: the DRS and a site that includes the MAP kinase insert. Previous reports have suggested that PEA-15 is not an inhibitor of ERK2; however, it is shown here to potently inhibit the ability of ERK2 to phosphorylate two transcription factors, Elk-1 and Ets-1, which contain docking sites for the DRS of ERK2. Therefore, in addition to sequestering ERK1/2 in the cytoplasm, PEA-15 has the potential to modulate the activity of ERK2 in cells by competing directly with proteins that contain D-sites.

The extracellular signal-regulated kinase 2 (ERK2)[1] cascade is activated by an array of external stimuli including growth factors, hormones, and neurotransmitters (*1*). Once initiated, the cascade plays important roles in a variety of cellular events such as proliferation, differentiation, and apoptosis (*2*, *3*). Involvement in such diverse cellular processes demands that this signal transduction pathway be strictly controlled. Failure to do so can result in inappropriate biological responses, some of which can be detrimental to the cell (*4*, *5*). Prior to stimulation, unactivated ERK2 is located predominately in the cytosol. As a result of cascade initiation, activated MKK1 phosphorylates ERK2 on Thr-183 and Tyr-185 and ERK2 redistributes in the cell. Depending on the cell stimulus and cell type, activated ERK2 may remain in the cell cytosol or move to the nucleus (*1*, *6*,

† This research was supported in part by the Welch Foundation (F-1390) and the NIH (GM59802). K.C. was a recipient of a NIH/NIEH predoctoral training grant (ES07247). Mass spectra were acquired by Dr. Herng-Hsiang Lo in the CRED Analytical Instrumentation Facility Core supported by NIEHS center grant ES07784. Molecular graphics images were produced using the UCSF Chimera package from the Resource for Biocomputing, Visualization, and Informatics at the University of California, San Francisco (supported by NIH P41 RR-01081).

* Corresponding author. Division of Medicinal Chemistry, College of Pharmacy, University of Texas at Austin, TX 78712. Tel: 512-4719267. Fax: 512-2322606. E-mail: Dalby@mail.utexas.edu.

‡ Graduate Program in Biochemistry, University of Texas at Austin.

§ Division of Medicinal Chemistry, University of Texas at Austin.

|| Stanford University.

⊥ Graduate Program in Molecular Biology, University of Texas at Austin.

[1] Abbreviations: 5-IAF, 5′-iodoacetamidofluorescein; BSA, bovine serum albumin fraction V; DTT, dithiothreitol; EDTA, ethylene diamine tetraacetic acid; EGTA, ethylene glycol-bis[2-aminoethyl ether]-*N*,*N*,*N*′,*N*′-tetraacetic acid; ERK, extracellular signal-regulated protein kinase; ESI, electrospray ionization; EtsΔ138, murine (His_6-tagged)-$Ets1^{1-138}$; HEPES, *N*-(2-hydroxyethyl)-piperazine-*N*′-2-ethanesulfonic acid; IPTG, isopropyl-β-D-thiogalactopyranoside; MAPK, mitogen-activated protein kinase; MKK1, MAP kinase kinase 1; MKP3, MAP kinase phosphatase 3; CAMKII, calmodulin-dependent protein kinase II; PKB, protein kinase B; PKC, protein kinase C; PEA-15*, PEA-15 labeled with fluorescein on Cys-27; P_{116}∼PEA-15*, PEA-15 labeled with fluorescein on Cys-27 and phosphorylated at Ser-116; P_{104}∼PEA-15*, PEA-15 labeled with fluorescein on Cys-27 and phosphorylated at Ser-104; PP∼PEA-15*, PEA-15 labeled with fluorescein on Cys-27 and phosphorylated at Ser-104 and Ser-116; k_a, the observed second-order rate constant for the alkylation of ERK2 mutants under native conditions; k'_a, the observed second-order rate constant for the alkylation of ERK2 mutants under native conditions in the presence of saturating ligand; ERK2-*CT*, an ERK2 protein containing a single cysteine target residue as well as a C-terminal PKA consensus sequence; CD domain, common docking domain usually designated as Asp-316 and Asp-319 of loop-16 in rat ERK2; DRS, D-recruitment site; FRS, F-recruitment site.

10.1021/bi700206u CCC: $37.00
Published on Web 07/21/2007

7), thus changing its proximity to cytosolic and/or nuclear substrates. By carefully controlling the extent and duration of the access given to ERK2, cells may control their ultimate response.

The regulation of ERK2 localization has been the subject of numerous studies (for recent examples see refs *8*−*11*). From these studies, it has been shown that the overexpression of ERK2 leads to its nuclear accumulation, and that cytosolic binding partners are important for its retention in the cytoplasm of quiescent cells. Accordingly, MKK1 was identified as a cytoplasmic anchor of ERK2, since coexpression of MKK1 and ERK2 in cells leads to the cytoplasmic retention of the overexpressed ERK2, even in the presence of activating stimuli (*12*). In addition to MKK1, experiments have identified several other cytoplasmic anchor proteins including Sef, β-arrestin, MKP3, PTP-SL, and Naf1α (*6*, *13*−*16*). Based on these and other studies, it has recently been suggested that the distribution of ERK2 may be explained by a simple binding equilibrium model (*10*, *17*). According to the model, the distribution of ERK2 is determined by ERK2−protein interactions occurring with binding partners located in both the cytosol and the nucleus. While this is an attractive model and can account for much of the observed localization, there is also evidence for an energy-dependent component to the regulation (*11*).

To construct meaningful models of ERK2 signal transduction pathways in cells, one requires knowledge of the complexes ERK2 forms, yet despite intense study relatively little is known about the protein−protein interactions that are mediated by ERK2. For example, no structure of ERK2 in complex with another protein has been reported, there is an absence of quantitative data regarding the strength of known ERK2−protein interactions, and the effect of post-translational modifications on these interactions is often poorly defined. ERK2−protein interactions may also be viable drug targets as indicated by the identification of several small molecule inhibitors that appear to inhibit docking interactions between ERK2 and several substrates (*18*, *19*).

One protein of particular interest that has been shown to regulate the distribution of ERK2 is phosphoprotein enriched in astrocytes-15 kDa (PEA-15). PEA-15 is a small anti-apoptotic protein expressed in a broad range of tissues and enriched in astrocytes (*20*). Several studies have demonstrated that PEA-15 is capable of binding to ERK2, although it is not a substrate (*21*, *22*). These same studies have also shown that the overexpression of PEA-15 prevents ERK2 from accumulating in the nucleus under conditions that normally favor nuclear localization, suggesting that one role of PEA-15 is to anchor ERK2 in the cytosol. In support of this notion, ERK2 was shown to be located predominantly in the nucleus of PEA-15 −/− astrocyte cells (*21*). Here we report that PEA-15 is a potent inhibitor of ERK2 that engages its D-recruitment site (DRS) as part of a tight bidentate interaction. Thus, not only does PEA-15 sequester ERK2 in the cytoplasm, it has the potential to inhibit the activity of ERK2 molecules that are accessible within the cytoplasm, potentially contributing to the specificity of the ERK2 signaling pathway.

EXPERIMENTAL PROCEDURES

Reagents

Ammonium hydroxide and TCA (trichloroacetic acid) were purchased from Fisher Scientific (Pittsburgh, PA). Ultrapure grade Tris was obtained from ICN Biomedicals (Aurora, OH). Sodium bicine, IAA (iodoacetamide), sodium deoxycholate, NTCB (2-nitro-5-thiocyanobenzoic acid), guanidine, catalytic subunit of protein kinase A, and other chemicals were obtained from Sigma (St. Louis, MO). MP Biomedicals (Irvine, CA) supplied [γ-^{32}P]-ATP. Yeast extract, tryptone, agar, and IPTG were obtained from US Biologicals (Swampscott, MA). Qiagen Inc. (Valencia, CA) supplied Ni-NTA agarose, Quiaprep Spin miniprep, PCR QIAquick Purification Kit, and QIAEX II Gel Extraction Kit. Restriction enzymes, PCR reagents, and T4 DNA ligase were from New England Biolabs (Beverly, MA) and Invitrogen Corp. (Carlsbad, CA). Oligonucleotides for DNA amplification and mutagenesis were from Genosys (Woodlands, TX). Mutagenesis reagents were purchased from Stratagene (La Jolla, CA). Ambion, Inc. (Austin, TX) provided the thin walled PCR tubes. The Mono Q HR 10/10 anion exchange column and PD-10 desalting columns were purchased from Amersham Biosciences (Piscataway, NJ). The *Escherichia coli* strain DH5α, used for cloning and mutagenesis, and the strains BL21 (DE3) and BL21(DE3)pLys, used for recombinant protein expression, were obtained from Invitrogen and Novagen (Madison, WI), respectively. The pET28a vector was purchased from Novagen.

General Methods

Techniques for restriction enzyme digestion, ligation, transformation, and other standard molecular biology manipulations were based on methods described by the manufacturer. Plasmids were introduced into cells using a BTX Transporter Plus. UV−vis absorbance readings were taken on a Varian Cary model 50 spectrophotometer. FPLC was performed on a Pharmacia ÄKTA FPLC system. HPLC was performed on a Waters HPLC system using a 250 mm × 4 mm Vydac RP C18 column (218TP54, reversed-phase material consists of octadecyl aliphatic groups bonded to the surface of 300 Å pore diameter silica). Protein was analyzed by Tris glycine sodium dodecyl sulfate−polyacrylamide gel electrophoresis (SDS−PAGE) under denaturing conditions on 10−15% gels using the Bio-Rad Mini-protean III vertical gel electrophoresis apparatus. The extinction coefficients (ϵ) for proteins were determined from the primary sequence, according to $\epsilon = 5690\ \text{cm}^{-1}\ \text{M}^{-1} \times$ (number of trp) + $1280\ \text{cm}^{-1}\ \text{M}^{-1} \times$ (number of tyr) + $120\ \text{cm}^{-1}\ \text{M}^{-1} \times$ (number of cys) (*23*) or in the case of ERK2 and Ets-1 by first determining the concentration of a protein solution by amino acid analysis. All mutants were verified by sequencing the DNA at UT core facilities using an Applied Biosystems automatic DNA sequencer.

Peptides. Peptides were synthesized at the UT Molecular Biology core facilities and additionally purified on a 250 mm × 22 mm Alltech Econosil C18 column (reversed-phase material consists of octadecyl aliphatic groups bonded to the surface of 60 Å pore diameter silica) developed with a linear gradient of 10−70% acetonitrile (containing 0.1% TFA (v/v)) over 35 min at 5 mL/min. The purified peptides were

raised in water and brought to pH 7.5 by the addition of sodium hydroxide. The concentration of each peptide was determined by amino acid analysis. The peptides used were Elk-1 F, *N*-AKLSFQFPS-*C* (1024 Da) (*24*), and Elk-1 D, *N*-QKGKRPRDLELPLSPSL-*C* (1934 Da) (*25*). The molecular weight of each peptide was determined by MALDI mass spectrometry.

Molecular Biology

Construction of pET28-His$_6$-PEA-15. Oligonucleotides: forward (5′-GG GAA TTC **CAT ATG** GCC GAG TAC GGG ACT CTC CTT C-3′) (*Nde*I site in bold) and reverse (5′-CCC **AAG CTT** TCA AGC CTT CTT TGG TGG GGG AGC C-3′) (*Hin*dIII site in bold) were used to generate the N-terminal hexahistidine tagged PEA-15 cleavable with thrombin. An amplification reaction (50 μL) contained Taq polymerase buffer, 200 μM each of the four deoxynucleoside triphosphates, 2 mM $MgCl_2$, 10 ng of template DNA (pQE9-PEA15 vector, a generous gift of Dr. Milton Werner), 1 μM primers forward and reverse, and 1 U of Taq DNA polymerase (TaKaRa Bio Inc., Japan). The cycling parameters were 94 °C for 30 s, followed by 30 cycles at 56 °C for 45 s, 72 °C for 1 min, 94 °C for 30 s with a final elongation step 72 °C for 10 min. The PCR product was digested with *Nde*I and *Hin*dIII, ligated into the *Nde*I−*Hin*dIII digested pET28a vector, and then transformed into DH5α *E. coli* cells. The construct was verified by sequencing the DNA at the UT core facilities using an Applied Biosystem automatic DNA sequencer.

Protein Expression, Purification, and Modification

Expression of (His$_6$-tagged) ERK1. Full length human ERK1 (a gift from Natalie Ahn) was cloned into an NpT7-5 vector (*26*), and the vector was electroporated into the *E. coli* strain BL21(DE3) (*26*). Cells were grown at 37 °C in Luria broth containing 50 μg/mL ampicillin to an optical density of 0.6, before being induced with 0.5 mM IPTG. The cells were then cultured for an additional 4 h at 30 °C. Cells were lysed in 150 mL of buffer A (40 mM Tris pH 7.0, 5 mM imidazole, 0.03% (by mass) Brij-30, 0.1% (v/v) β-mercaptoethanol, 1 mM benzamidine, 0.1 mM PMSF, and 0.1 mM TPCK) containing 0.75 M NaCl and 1% (by mass) Triton X-100. The suspension was sonicated for 20 min (at 5 s pulses with 5 s intervals) at 4 °C. The lysate was cleared (16000 rpm, 25 min, 4 °C) and the supernatant agitated gently with 3 mL of Ni-NTA beads (Qiagen). The beads were washed with 150 mL of buffer A (pH 7.5), and the His$_6$-ERK1 was eluted with 100 mL of buffer A (pH 8.0) containing 200 mM imidazole. The eluted protein was loaded onto a Mono Q HR 10/10 anion exchange column that had been pre-equilibrated in buffer B (20 mM Tris pH 8.0, 0.03% (by mass) Brij-30, and 0.1% (v/v) β-mercaptoethanol). The column was developed with a gradient of 0−500 mM NaCl over 17 column volumes, and the protein was eluted at 225−250 mM NaCl. Collected fractions were combined and dialyzed into buffer C (50 mM sodium phosphate buffer pH 7.0, and 0.1% (v/v) β-mercaptoethanol). Following dialysis, the protein was loaded onto a Mono S HR 5/5 cation exchange column that had been pre-equilibrated in buffer C containing 0.03% (by mass) Brij-30. The column was developed with a gradient of 0−500 mM NaCl over 17 column volumes, and the protein was eluted at 15−40 mM NaCl. Collected fractions were combined and dialyzed into buffer D (25 mM HEPES pH 7.5, 50 mM KCl, 0.1 mM EDTA, 0.1 mM EGTA, and 2 mM DTT). The concentration of activated ERK1 was established using the calculated extinction coefficient (A_{280}) of 40830 cm^{-1} M^{-1}.

Activation of (His$_6$-tagged) ERK1. ERK1 was incubated with MKK1G7B (20:1 mole ratio) in buffer E (25 mM HEPES pH 7.5, 20 mM $MgCl_2$, 2 mM DTT, 0.5 mM EGTA) containing 4 mM ATP. After 3 h, the buffer was exchanged with buffer B to remove the ATP. The sample was then loaded onto a Mono Q HR 5/5 column. A linear gradient of 0−500 mM NaCl was applied, and the protein eluted at 300−325 mM NaCl. The fractions were collected and dialyzed overnight into storage buffer (buffer F) (25 mM HEPES pH 7.5, 50 mM KCl, 2 mM DTT, 0.1 mM EDTA, 0.1 mM EDTA, and 10% glycerol). The protein was concentrated to ∼150 μM using an Amicon Ultra-15 centrifugal device (Millipore). The phosphorylation of ERK1 was confirmed by ESI mass spectrometry following elution (0−100% acetonitrile, 80 min, 0.6 mL/min) from a reverse phase C18 Vydac column (218TP54, 25 cm × 4 mm).

Expression and Purification of PEA-15. Full length PEA-15 used for fluorescence spectroscopy experiments was cloned into the pQE-9 vector (*22*), while PEA-15, used for footprinting purposes, was cloned into pET28a to provide a cleavable His$_6$-tag. The pQE-9 construct was co-transformed into BL21(DE3) cells with the pREP4 vector, while the pET28a construct was transformed on its own. The expressions and purification of both proteins were conducted following similar protocols: Cells were grown at 37 °C in Luria broth containing 50 μg/mL ampicillin and 25 μg/mL kanamycin to an optical density of 0.6 before being induced with 0.5 mM IPTG. The cells were cultured for an additional 4 h at 30 °C before being harvested. PEA-15 was purified in a manner similar to ERK1, with elution from the Mono-Q column occurring at 98 mM NaCl. 65 mg of purified PEA-15 per liter of culture was concentrated to ∼1.3 mM using an Amicon Ultra-15 centrifugal device. The concentration was established using the extinction coefficient (A_{280}) of 10930 cm^{-1} M^{-1}.

His$_6$-tag Cleavage. His$_6$-PEA-15 expressed from pET28a has an N-terminal sequence of Met-Gly-Ser-Ser-His-His-His-His-His-His-Ser-Ser-Gly-Leu-Val-Pro-Arg-Gly-Ser-His prior to the initial methionine encoded by PEA-15. To remove the hexahistidine tag, His$_6$-PEA-15 (30 mg) was subjected to thrombin proteolysis in 30 mL reaction volume containing 10 units of thrombin. The cleavage was carried out for 5 h at 25 °C in cleavage buffer (buffer G) (20 mM Tris, 150 mM NaCl, 2.5 mM $CaCl_2$). The reaction sample was then dialyzed into buffer B at 4 °C and applied to a Mono Q HR 10/10 anion exchange column. The collected fractions were combined and dialyzed into buffer D. Cleavage of the His$_6$-tag was confirmed by SDS−PAGE and mass spectrometry. The concentration was established using an extinction coefficient (A_{280}) of 10930 cm^{-1} M^{-1} for PEA-15.

Alkylation of PEA-15. Cys-27 of the cleaved PEA-15 was subjected to alkylation with iodoacetamide in a reaction mixture containing 100 mM bicine, pH 8.6 and 20 mM iodoacetamide (40-fold excess), at 25 °C for 8 h in the dark (*27*). The reaction was stopped by the addition of a 10-fold molar excess of β-mercaptoethanol, and then the alkylated

protein was loaded immediately onto a Mono Q HR 10/10 anion exchange column, pre-equilibrated in buffer B. The eluted fractions of PEA-15 were collected, dialyzed into buffer F, and concentrated using an Amicon Ultra-15 centrifugal device.

Phosphorylation of PEA-15 by PKC or CAMKII. Before phosphorylation, 3 mg of PEA-15 was dialyzed overnight at 4 °C into 25 mM HEPES pH 7.5 and 2 mM DTT to ensure that all EDTA and EGTA were removed since EDTA and EGTA could bind essential calcium needed for PKC and CAMKII activity. The phosphorylation of PEA-15 by PKC was carried out at 27 °C for 4 h in 20 mM HEPES pH 7.5, 2 mM DTT, 5 mM $MgCl_2$, 100 μM $CaCl_2$, 1 X PKC lipid activator (Upstate Biotechnology), 1 mM ATP, 300 μM PEA, and 180 nM PKC βII in a final volume of 400 μL. The phosphorylation of PEA-15 (300 μM) by CAMKII (10000 U/mL) was carried out at 30 °C for 6 h in buffer G (20 mM Tris pH 7.5, 0.5 mM DTT, 10 mM $MgCl_2$, 2 mM $CaCl_2$, 2.4 μM calmodulin, 1 mM ATP) in a final volume of 560 μL. After activation, reactions were stopped with 10 mM EGTA and then dialyzed overnight at 4 °C in 20 mM Tris pH 8.0, and 0.1% β-mercaptoethanol (v/v). The protein was loaded onto a Mono Q HR5/5 anion exchange column. A gradient of 0−500 mM NaCl was applied over 17 column volumes to elute the protein at 355−410 mM NaCl. The fractions were pooled and dialyzed overnight at 4 °C in buffer F (minus glycerol). The single phosphorylation of PEA-15 was confirmed by ESI mass spectrometry following elution (0−100% acetonitrile, 80 min, 0.6 mL/min) from a reverse phase C18 Vydac column (218TP54, 25 cm × 4 mm).

Preparation of Fluorescein-Labeled PEA-15. Because PEA-15 contains a single cysteine, it can easily be labeled with fluorescein. Using 5′-iodoacetamidofluorescein (5-IAF), a fluorescein moiety was covalently linked to cysteine 27 through a thioether linkage. Prior to reaction with 5-IAF, the protein was dialyzed overnight at 4 °C into 2 L of buffer H (20 mM HEPES pH 7.3, 50 mM KCl, and 2 mM EDTA) to remove DTT. A fresh stock of 10 mM 5-IAF was made in dimethylformamide (DMF) and kept in the dark. The stock concentration was determined by measuring the absorbance at 492 nm (ϵ_{492} = 78000 cm^{-1} M^{-1}). Since the absorption of fluorescein is pH sensitive, the absorbance readings were made in 20 mM HEPES pH 7.5. To initiate the labeling reaction, 5-IAF (10:1 mole ratio) was added dropwise to a solution of the protein in labeling buffer. The reaction was allowed to proceed overnight at 4 °C in the dark. After 13−14 h, the reaction was quenched by addition of a 10-fold molar excess of β-mercaptoethanol. The sample was then concentrated to a volume of 2.5 mL and applied to a PD-10 desalting column (Amersham) to remove any unreacted 5-IAF. The labeled protein was further purified by anion exchange chromatography using a Mono Q HR 10/10 column. Unlabeled protein eluted at 150 mM, and the fluorescein-labeled protein eluted at 225 mM NaCl. The collected fractions were dialyzed overnight at 4 °C in buffer D. Labeling of the protein was verified by ESI mass spectrometry following elution (0−100% acetonitrile, 80 min, 0.6 mL/min) from a reverse phase C18 Vydac column (218TP54, 25 cm × 4 mm).

Fluorescence Spectroscopy

To investigate the spectral properties of the PEA-15*, P_{116}∼PEA-15*, P_{104}∼PEA-15* and PP∼PEA-15*, 100 nM of the protein was examined in buffer I (25 mM HEPES pH 7.5, 50 mM KCl, 40 μg/mL BSA, 0.1 mM EDTA, 0.1 mM EGTA, 1.3% glycerol, and 2 mM DTT) in a final volume of 60 μL. Fluorescence measurements were made at 27 °C using a Fluorolog model FL3-11 fluorometer (Jobin Yvon, Edison, NJ) using three-window fluorescence grade quartz cuvettes with a 1.0 cm path length and 55 μL aqueous volume purchased from Hellma (Plainview, NY). In order to determine the excitation maximum, an excitation scan was performed from 450 to 500 nm. Slit widths were set to 1 nm, the integration time for each reading was 500 ms, and the emission was monitored at 517 nm. For determination of the emission maximum, fluorescein-labeled proteins were excited at 492 nm and an emission scan was performed from 500 to 600 nm. Slit widths were set to 2.5 nm, and the integration time for each reading was 500 ms. To determine the effect of binding on the fluorescent yield, the fluorescence emission was examined in the absence and presence of 20 μM ERK2. The resulting peaks on the emission scans were then integrated to determine the ratio of the fluorescence yield of the bound fluorophore to the free fluorophore, *R*. *R* was also calculated from the anisotropy experiments by measuring the polarized intensities for the free and bound forms of the fluorophore, according to the equation $R = (I_V + 2GI_H)_{bound}/(I_V + 2GI_H)_{free}$, where I_V and I_H are the intensity of the emission at polarizations both parallel and perpendicular to the excitation source and *G* is a factor to correct for instrumental differences in detecting emission components. Specifically, the *G* factor is the ratio of the intensity of the vertically and horizontally polarized emission components when the sample is excited with horizontally polarized light. The program Instrument Control Center (Jobin Yvon, Edison, NJ) was used to collect data and to calculate the fluorescence anisotropy, *r*, which is defined as $r = (I_V - GI_H)/(I_V + 2GI_H)$. In this case the protein was excited with polarized light at 492 nm and the horizontal and vertical components of the emitted light were detected at 515 nm. Excitation and emission slit widths were set to 5 nm, and the integration time for each reading was 300 ms. Measurements were taken every 15 s for a total of 3 min, and the resulting anisotropy values were averaged.

$$r = \frac{\frac{K_d + [S_t] + [E_t] - \sqrt{(-K_d - [S_t] - [E_t])^2 - 4[E_t][S_t]}}{2[S_t]}(r_b R - r_f) + r_f}{1 + \frac{K_d + [S_t] + [E_t] - \sqrt{(-K_d - [S_t] - [E_t])^2 - 4[E_t][S_t]}}{2[S_t]}(R - 1)} \quad (1)$$

The dissociation constants were determined by fitting the average anisotropy values to eq 1 using Kaleidgraph 3.6 (Synergy software). Here r_f and r_b are the anisotropies of the free and bound fluorescein-labeled protein, *R* is the ratio of fluorescent yields of the bound form and the free form, $[S_t]$ and $[E_t]$ are the total concentrations of the fluorescein-labeled protein and enzyme, and K_d is the dissociation constant. For fluorescence anisotropy competition assays the

average anisotropy values were calculated and fit using eqs 2−6 in Scientist (Micromath).

$$r = \frac{\frac{[ES]}{[S_t]}(r_b R - r_f) + r_f}{1 + \frac{[ES]}{[S_t]}(R - 1)} \quad (2)$$

$$[ES] = \frac{[E_f][S_f]}{K_d + [E_f]} \quad (3)$$

$$K'_d = \frac{[E_f][B_f]}{[EB]} \quad (4)$$

$$B_t = B_f + EB \quad (5)$$

$$E_t = E_f + EB \quad (6)$$

Cysteine Footprinting

30−50 μg of His_6-ERK2, containing a single cysteine and a C-terminal PKA site (an ERK2-*CT*), was radiolabeled for 15 min at 37 °C in 50 mM Tris, pH 7.5, 10 mM $MgCl_2$, 1 U of catalytic subunit of protein kinase A, 4 mM DTT, 1 μM unlabeled ATP, and 10 μCi [γ-^{32}P]-ATP (7000 Ci/mmol). The enzymatic activity of the PKA was quenched by the addition of 5 μM PKI, a potent inhibitor of PKA (*28*). Cysteine footprinting experiments were performed in the presence or absence of alkylated PEA-15 (0.5 mM) following methods described for EtsΔ138 in the preceding paper (*29*).

Enzyme Kinetics

Elk-1 Phosphorylation. Inhibition assays were performed at 27 °C in assay buffer E containing 2 nM activated ERK2, 4 μM GST-Elk1 (residues 307−428), and 300 μM [γ-^{32}P]-ATP at varied PEA-15 concentrations (0, 2.5, and 25 μM) in a total volume of 100 μL. The reactions were incubated for 5 min before initiation by addition of [γ-^{32}P]-ATP. Aliquots (10 μL) were taken and immediately heated for 3 min at 100 °C. These samples were then run on a 10% SDS−PAGE gel. After being stained, the gel was exposed to phosphor screens (Molecular Dynamics) and the amount of radiolabeled phosphorylated Elk-1 was determined using the program ImageQuant (Molecular Dynamics).

EtsΔ138 Phosphorylation. Assays were carried out at 6 μM EtsΔ138 using varied concentrations of PEA-15 (0−250 nM). The reactions (100 μL final volume) were incubated for 5 min before initiation by addition of [γ-^{32}P]-ATP. Aliquots (10 μL) were taken at time points and applied to P81 cellulose paper (2.5 × 2.5 cm). Rates were measured under conditions where total product formation represented less than 10% of the initial substrate concentration. The P81 papers were first washed in 50 mM phosphoric acid (5 × 10 min) and then in acetone (1 × 10 min). After the papers were dry, the amount of radiolabeled protein was determined by counting the associated cpm on a scintillation counter. All data was processed using the program KaleidaGraph 3.6 (Synergy Software). Initial rates were determined by fitting plots of product against time to the equation of a straight line.

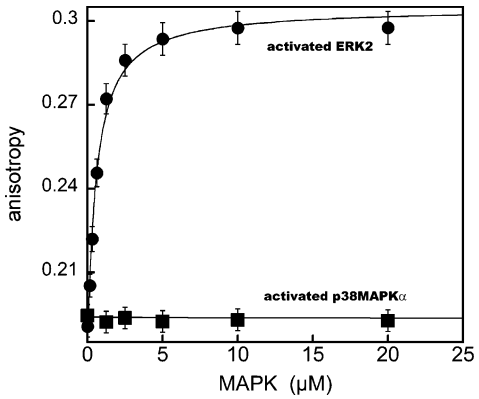

FIGURE 1: Binding of PEA-15* to activated ERK2 and p38MAPKα. Binding of 100 nM PEA-15* to 0−20 μM activated ERK2 (●) or activated p38MAPKα (■). Anisotropy values were averaged and the dissociation constants were determined by fitting the average anisotropy values (reproducible to within 2%) to eq 1 using an *R* value of 1.0 (see Table 1).

RESULTS AND DISCUSSION

The ERK1/2·PEA-15 Complex Is Not Regulated by Phosphorylation

PEA-15 is a small anti-apoptotic protein that is involved in a variety of cellular processes (*30*−*33*). In many of these processes it exhibits an effect on the ERK1/2 signal transduction pathway (*30*−*32*). Accordingly, multiple studies have shown that PEA-15 binds ERK1/2, causing it to be sequestered in the cytoplasm (*21*), thereby regulating the outcome of the ERK1/2 signaling program. When PEA-15 was first discovered in astrocytes, it was found to exist in three different forms, unphosphorylated, monophosphorylated, and diphosphorylated (*34*). The monophosphorylated forms correspond to phosphorylation at either Ser-104 or Ser-116, while the diphosphorylated form is phosphorylated at both sites (*20*, *34*). The phosphorylation of Ser-116 is accomplished by CAMKII (and PKB) (*34*) and Ser-104 by PKC (*20*). Conflicting functions for the phosphorylation of Ser-104 have been reported with one study suggesting that its phosphorylation destabilizes the binding of ERK2 (*35*), while another study suggests that it has no direct effect (*36*). As ERK2 must locate to the nucleus to facilitate cell division, it is critical to understand how its interactions with cytoplasmic proteins such as PEA-15 are regulated. To address this issue and also to quantify the affinity of PEA-15 for both ERK1 and ERK2, PEA-15 was overexpressed in *E. coli* and then labeled by a fluorescein moiety on Cys-27 (see Experimental Procedures).

Relative to ERK2, which is 42 kDa and monomeric under the conditions employed (*37*), PEA-15 is a small 15 kDa protein and, therefore, when labeled with a suitable flurophore it is predicted to furnish an observable change in fluorescence anisotropy upon binding ERK2. To examine the binding of MAPKs to PEA-15, a 100 nM solution of fluorescein-labeled PEA-15 (PEA-15*) was added to varying concentrations of activated and unactivated ERK1, ERK2, or p38 and the resulting anisotropy measured. The anisotropy values increased with the addition of ERK1 and ERK2, but not p38 MAPK (see Figure 1 for representative plots showing the binding of PEA-15 to activated ERK2 and p38 MAPKα). Thus, as shown previously (*21*), ERK1/2, but not p38MAPK,

Table 1

ERK	PEA-15	phosphorylation site	K_d, nM unactivated ERK	K_d, nM activated ERK
ERK1	PEA-15		182 ± 10^b	245 ± 24^b
ERK1	PEA-15*		48 ± 10^a	550 ± 50^a
ERK1	P∼PEA-15*	116	41 ± 16^a	462 ± 60^a
ERK1	P∼PEA-15*	104	51 ± 16^a	670 ± 70^a
ERK1	PP∼PEA-15*	104, 116	50 ± 15^a	600 ± 80^a
ERK2	PEA-15		133 ± 5^b	130 ± 42^b
ERK2	PEA-15*		62 ± 18^a	460 ± 80^a
ERK2	P∼PEA-15*	116	39 ± 12^a	400 ± 75^a
ERK2	P∼PEA-15*	104	48 ± 14^a	540 ± 83^a
ERK2	PP∼PEA-15*	104, 106	45 ± 15^a	630 ± 120^a

[a] Determined from fluorescence anisotropy binding assays. [b] Determined from fluorescence anisotropy competition assays

form a complex with PEA-15. Fitting the binding data to a simple binding model furnished dissociation constants of K_d ∼50 nM and 500 nM for the unactivated and activated enzymes, respectively (Table 1).

Effect of ERK1/2 Phosphorylation on PEA-15 Binding. To determine the affinity of unlabeled PEA-15 for ERK1/2, it was allowed to compete with PEA-15* for binding to ERK1/2. The expected decrease in anisotropy, which accompanied the dissociation of PEA-15* from ERK1/2, was analyzed according to eq 2−6, which furnished dissociation constants of $K_d = 180 \pm 10$ nM and 250 ± 30 nM for ERK1 and ERK1-PP, respectively (data not shown). Similar values were obtained for ERK2 (see Table 1). These data established that PEA-15 is a tight binding ligand for the ERK1/2 proteins whose affinity is not regulated by their MKK1 mediated phosphorylation. The analysis also shows that the fluorescein moiety on Cys-27 slightly influences the affinity of each complex: unactivated ERK1/2 binds 3−4-fold more tightly to the labeled protein, while activated ERK1/2 binds 2−3-fold more weakly (Table 1). Thus, both pull-down experiments (*21*) and those reported here show that PEA-15 binds both activated and unactivated ERK2, prompting the question of how the interaction is regulated *in vivo*.

Effect of PEA-15 Phosphorylation on ERK1/2 Binding. As the effect of introducing the fluorescent label was found to be relatively minor, PEA-15* was used to examine whether the phosphorylation of PEA-15 regulates the stability of the ERK1/2·PEA-15 complex. Therefore, following purification from the bacterial lysate (Ni-NTA affinity chromatography and anion exchange chromatography) PEA-15 was phosphorylated by incubation with the appropriate Ser-104 and/or Ser-116 protein kinase. After verification of the final stoichiometry of phosphorylation by mass spectrometry, the fluorophore was attached to Cys-27 and the labeled protein purified (see Experimental Procedures). The binding affinities of each phospho-PEA-15* was examined in an identical manner to PEA-15*. The analyses (not shown) indicated that none of the phosphorylations (phosph-104, phospho-116 and phospho-104/116) had an effect on the affinity of PEA-15* for ERK1/2 (Table 1).

Thus, the phosphorylation of neither ERK1/2 nor PEA-15 appears to significantly influence the affinity of the ERK1/2·PEA-15 complex. This is consistent with a recent suggestion that the phosphorylation state of PEA-15 might control its interactions with other proteins. In support of this idea, the phosphorylation of PEA-15 has been reported to promote its binding to FADD (*35*). Through such a scenario the availability of PEA-15, to bind ERK1/2, may be regulated.

PEA-15 Binds the DRS of ERK2

Displacement of PEA-15 from ERK1/2 by a D-Site Peptide.[2] ERK2/p38 MAPK chimeras were previously used to identify a binding site for PEA-15 on ERK1/2, which was confirmed by the use of site-directed mutagenesis and pull-down assays (*38*). These studies identified a patch of several residues that precede the αG helix and several within the MAPK insert that are critical for PEA-15 binding (P1 site in Figure 2A,C). In addition to the P1 site on ERK2, two sites on PEA-15 were found to be important for binding ERK2 (*22*). The E1 site corresponds to several residues in the N-terminal death effector domain (DED) of PEA-15, while the E2 site corresponds to a distinct series of residues in the C-terminus (Figure 3). Both sites were first identified by NMR footprinting and then shown by site-directed mutagenesis to be critical for ERK2 binding (*22*). The E2 site is intriguing, because it lies at the end of a flexible tail with the potential to form a discrete interface with ERK2. Significantly, the critical residues in the E2 site, ^{121}I-K-L-A-P−P−P-K-K^{129} (which are underlined), are reminiscent of the sequence (R/K)$_{2-3}$-X$_{4-6}$-Φ_A-X-Φ_B, the consensus binding sequence for the D-recruitment site (DRS) of ERK2. However, rather than conforming to this sequence exactly, the E2 site corresponds to the consensus sequence in the reverse direction (*25*, *39*, *40*). The DRS is a hydrophobic groove on the rear face of ERK2 (see Figure 2A,B for a surface representation), formed by the α_D and α_E helices, loop-8, loop-11, and the β_7 and β_8 strands. At the end of the groove, distal to the active site is loop-16, which contains the CD site (Asp-316 and Asp-319) (Figure 2B). Basic residues of a D-site often make complementary interactions with acidic residues on loop-16, and one or both of the hydrophobic residues of the Φ_A-X-Φ_B motif are usually located at the $\varnothing_1$ or $\varnothing_2$ sites (Figure 2B).

Recently, the peptide *N*-QKGRKPRDLELPLSPSL-*C*, derived from the D-site of Elk-1, was shown to bind the DRS of ERK2 (*29*). To test the possibility that PEA-15 also binds the DRS, the ability of this peptide to compete against PEA-15 for the binding to ERK2 was assessed. The assay contained 100 nM PEA-15* and excess ERK2 at a concentration that was sufficient to ensure the formation of the ERK2·PEA-15 complex in the absence of a competitor. The Elk-1 D-site peptide was then added over a range of concentrations (0−170 μM) and the anisotropy of the solution determined. The addition of increasing amounts of the peptide resulted in a decrease in the anisotropy of the solution for both activated (Figure 4) and unactivated ERK2 (data not shown). The data were analyzed according to a competitive model and fit to eqs 2−6 using an *R* value of 1.0 and the appropriate dissociation constants for the ERK1/2·PEA-15* complexes. The line through the data in Figure 4 corresponds to the best fit to the competitive model and furnishes a dissociation constant of 3.9 ± 0.2 μM for the

[2] Two docking sites have been identified on MAPK ligands. One is called a D-site and is recognized by the D-recruitment site (DRS). The other is called an F-site and is recognized by the F-recruitment site (FRS). D-sites have also been called DEJL-domains, while F-sites have also been called DEF domains or Phe-X-Phe domains.

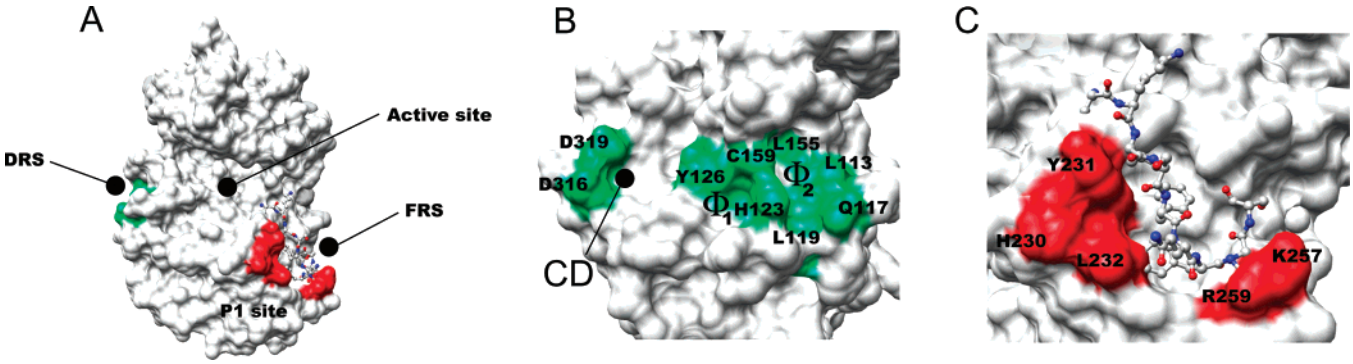

FIGURE 2: Binding interfaces of the ERK2·PEA-15 complex. A. Surface representation of activated ERK2 (PDB 4ERK) showing the P1 site, which contains residues critical for PEA-15 binding (red). The DRS and FRS are also indicated. B. Expanded view of the DRS with residues substituted for cysteine labeled and highlighted in green. C. Magnified view of the FRS with the peptide sequence AKLSFQFPS shown bound. This sequence was modeled in as part of the longer peptide PRSPAKLSFQFPS (*44*).

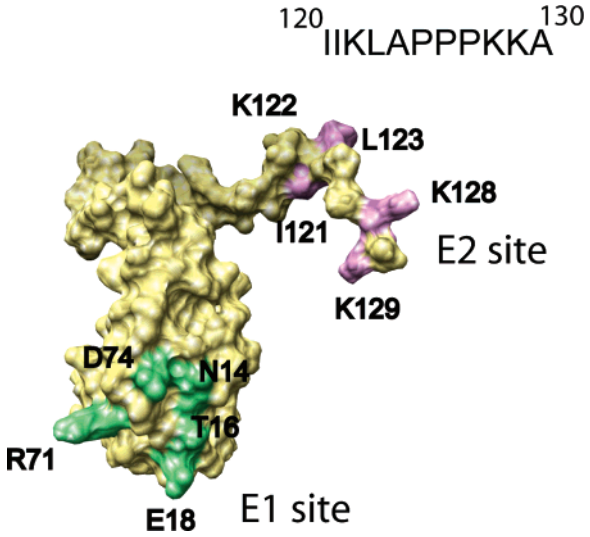

FIGURE 3: Surface representation of PEA-15. Surface representation of PEA-15 (PDB 1N3K) showing the E1 site and the E2 site with residues critical for ERK2 binding labeled and highlighted (E1, green; E2, plum).

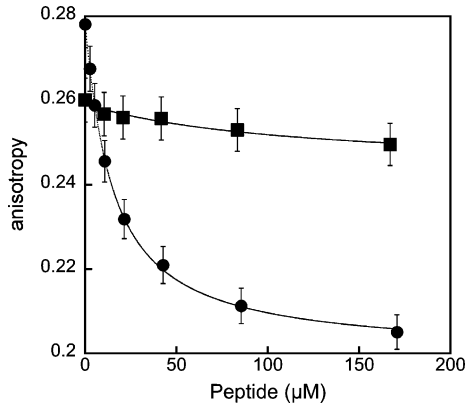

FIGURE 4: ERK2 displacement of PEA-15* from ERK2 by a D-site and F-site peptides. The competition assay (●) contained 100 nM PEA-15*, 0−171 μM Elk-1 D peptide, and 1.25 μM activated ERK2. The competition assay (■) contained 100 nM PEA-15*, 0−171 μM Elk-1 F-peptide (AKLSFQFPS), and 625 nM activated ERK2. Experimental data (reproducible to within 2%) were plotted and fit to eqs 2−6 using an R value of 1.0 and a dissociation constant for the ERK2·PEA-15* complex of $K_d = 0.46$ μM.

binding of the D-site peptide to activated ERK2. We argue, in the preceding paper, that the reason for the competition between the D-site peptide and the substrate Ets-1 is that they both bind the DRS of ERK1/2 (*29*). The same arguments may be applied to the case of PEA-15 also.

Table 2

secondary structure	site	ERK2-*CT*	k_a M^{-1} s^{-1}	fold protection k_a/k'_a
αD helix	$Ø_2$	L113C	0.09 ± 0.01	9.5 ± 1.4
loop-8	$Ø_2$	Q117C	6.5 ± 0.5	1.1 ± 0.2
loop-8	$Ø_2$	L119C	0.65 ± 0.05	1.1 ± 0.2
αE helix	$Ø_1$ and $Ø_2$	H123C	19.0 ± 1.0	1.0 ± 0.2
αE helix	$Ø_1$	Y126C	2.1 ± 0.1	1.1 ± 0.2
β7 sheet	$Ø_2$	L155C	0.04 ± 0.008	5.0 ± 1.5
loop-11	$Ø_1$ and $Ø_2$	C159	1.8 ± 0.2	29.0 ± 4.0
loop-16	CD	D316C	0.6 ± 0.1	0.9 ± 0.2
loop-16	CD	D319C	0.5 ± 0.1	1.3 ± 0.2
αG helix	P1	L232C	33.0 ± 1	110.0 ± 2.0

Cysteine Footprinting. As part of a program toward understanding the catalytic mechanism of ERK2, we developed a method for identifying ligand interactions at its DRS, which is described in the preceding paper (*29*). This approach employs forms of ERK2 containing a single cysteine residue and a C-terminal consensus sequence for PKA that can be radiolabeled using [γ-^{32}P]-ATP (*29*). These proteins are called ERK2 cysteine targets (ERK2-*CTs*) whose use exploits both the relative inflexibility of the ERK2 DRS and the sensitivity of cysteine alkylation rates to their protein environment (*29*). Comparisons between various structures of ERK2 (activated ERK2, unactivated ERK2, and two complexes of unactivated ERK2 bound to D-site peptides (*41*−*43*)) reveal extensive differences in the structure of the activation loop, but minor change in the structure of the DRS. These observations suggest that very little change in the protein environment of the DRS is expected to result from a conformational change induced by ligand binding, but rather any change is expected to be the consequence of a new DRS−ligand interface. Thus, by comparing the rate of alkylation of ERK2-*CTs*, which contain cysteines in the DRS, in the presence and absence of a ligand such as PEA-15, one can deduce whether the ligand binds the DRS directly.

To explore the possibility that PEA-15 binds the DRS, the alkylation of the ERK2-*CTs*, described in Table 2, was examined in the presence and absence of a saturating concentration of PEA-15 (312 μM), following the protocol described in the preceding paper (*29*) (see also Figure 2B, which indicates the residues for which ERK2-*CTs* were

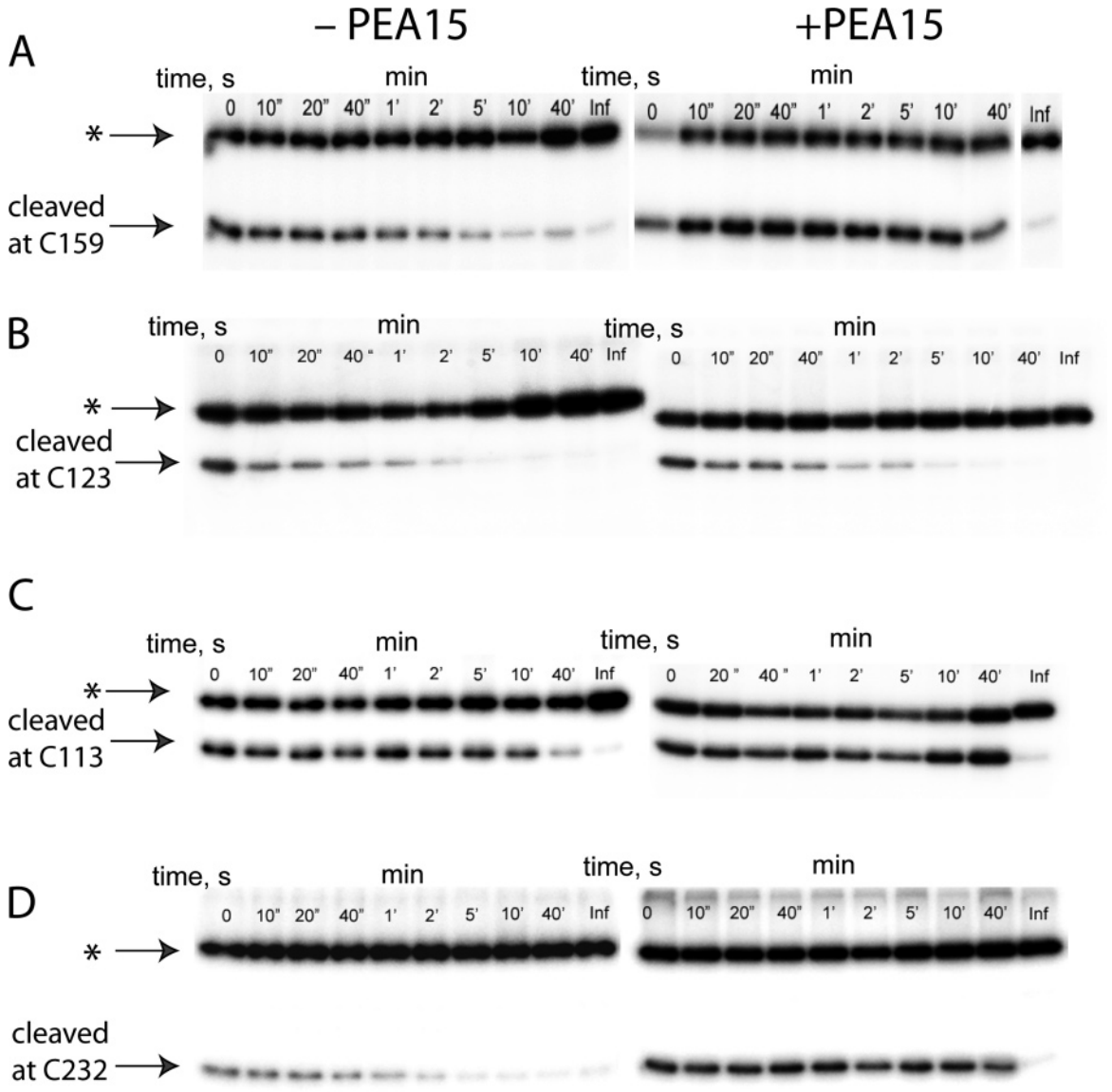

FIGURE 5: Cysteine footprinting of the ERK2 and PEA-15·ERK2 complexes. C-terminally radiolabeled single cysteine ERK2 mutants (C159, H123C, L113C, and L232C) were alkylated by iodoacetamide at pH 8.3 and 23 °C in the absence and presence of 313 μM PEA-15. At the times indicated, 30 μL aliquots were quenched with excess DTT, and the ERK2 was separated from excess PEA-15 (where necessary), denatured, and then cyanylated with excess (25 mM) 2-nitro-5-thiocyanobenzoic acid (NTCB). The cyanylated proteins were precipitated, washed, resuspended, and cleaved in 0.6 M NH_4OH. Samples were then fractionated by 15% SDS−PAGE, the gels dried, and the bands quantified on a Phosphorimager (see Experimental Procedures). The lanes correspond to the time when an aliquot was taken. The upper band corresponds to uncleaved ERK2, and the lower band corresponds to the labeled C-terminal fragment.

generated and analyzed). Figure 5 shows a typical set of SDS−PAGE gels used to analyze the rates of ERK2-*CT* alkylation. At various time points following the initiation of the alkylation reaction an aliquot was taken and analyzed by NTCB-mediated cleavage. The slower running band in each lane (*) corresponds to uncleaved ERK2-*CT*, resulting from either alkylation or β-elimination of the cyanylated protein (*29*). The faster running protein band in each lane (cleaved as indicated) corresponds to the C-terminal half of each cleaved ERK2-*CT*. To determine the rate of alkylation, the relative level of radioactivity associated with the cleavage product (the lower band) was determined by phosphorimage analysis. After exhaustive alkylation a small trace of the cleaved ERK2-*CT* is detectable in most lanes (lane labeled Inf), which probably reflects a minor misfolded population of the ERK2-*CT* that cannot be alkylated. In the presence of an excess of iodoacetamide [0.5−10 mM], the cleavage products were found to disappear following a pseudo-first-order rate law. Figure 6 shows several representative time courses where the *relative density* of the band associated with each cleaved ERK2-*CT* is plotted against time. Second-order rate constants for ERK2-*CT* alkylation were calculated from a minimum of two replicate experiments using different preparations of each ERK2-*CT*. The sensitivity of the footprinting analysis is such that a 2-fold difference in a rate constant for alkylation may be determined readily. Of the ERK2-*CTs* tested, three, L113C, L155C, and C159, which form part of the $Ø_2$ site (Figure 2B), exhibited a 5−29-fold retardation in their rate of alkylation upon the binding of PEA-15, while the rest were essentially unaffected (Table 2). These data are consistent with the notion that PEA-15 binds the $Ø_2$ site of the DRS. Interestingly, the extent of

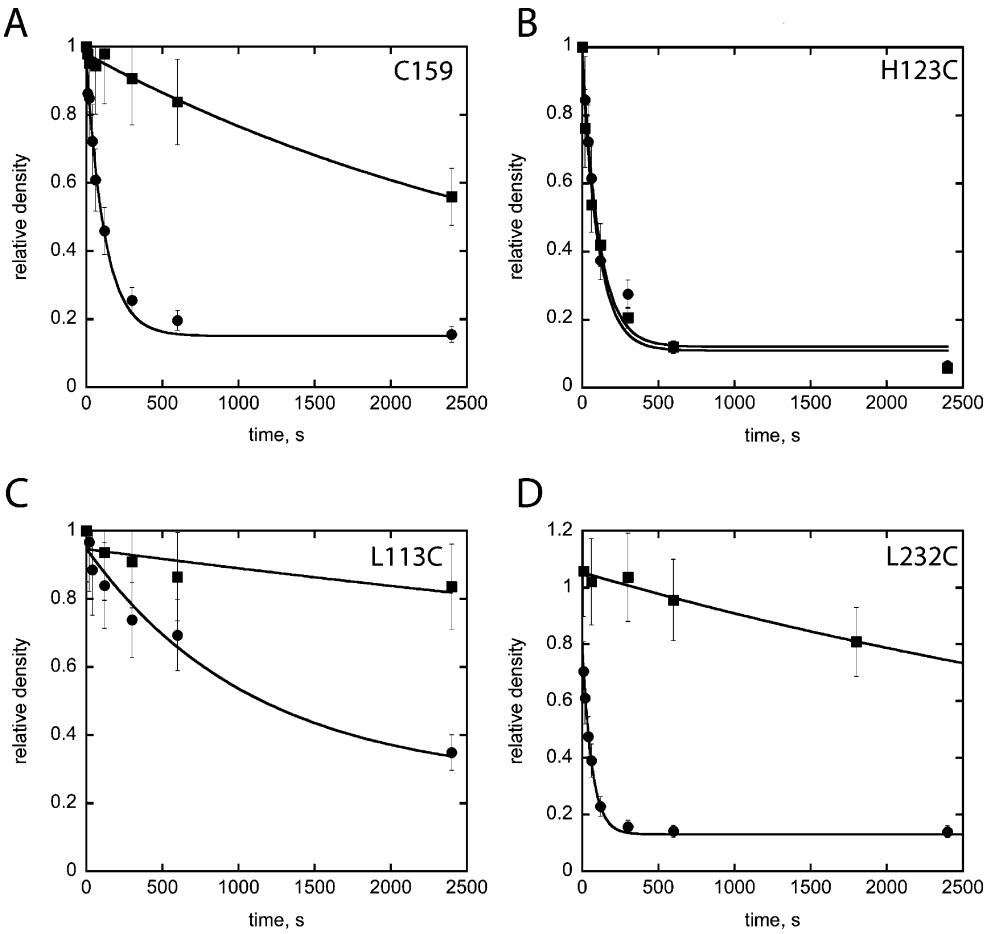

FIGURE 6: Alkylation of ERK2-*CTs* versus time for in the presence and absence of PEA-15. Representative plots (A−D) showing the time course for the disappearance of unalkylated ERK2-*CTs* (measured by the presence of NTCB-mediated cleavage product) in the presence (●) and absence (■) of 0.5 mM PEA15. The relative density of each gel quadrant containing a band associated with the ERK2-*CT* cleavage product was determined at various time points by phosphorimage analysis of gels similar to those shown in Figure 5 (see Experimental Procedures). The line through the data corresponds to the best fit to a first-order rate law (reproducible to within 30%). Endpoints used to determine rate constants for each alkylation reaction were determined after more than 10 half-lives. Some variability in the relative densities of the endpoints is seen between experiments, which reflect variability in the background radioactivity of the gel quadrants used to determine the relative densities. Replicate experiments were performed on a minimum of two different preparations of ERK2-*CT*. The sensitivity and reproducibility of the footprinting analysis is such that a 2-fold difference in a rate constant for alkylation may be readily determined. Rate constants and errors are reported in Table 2.

protection PEA-15 affords the ERK2-*CT* Cys-159 is identical to that afforded by the binding of the D-site peptide QKGRKPRDLELPLSPSL (*29*), providing good evidence that PEA-15 and the peptide compete for the same DRS binding site on ERK2. In fact, Figure 7 reveals that the overall pattern of protection induced by the peptide and PEA-15 are very similar, suggesting that their modes of binding are comparable.

PEA-15 Is Not Displaced from ERK1/2 by an F-Site Peptide

Previous NMR and mutagenesis experiments showed that residues His-230, Tyr-231, and Leu-232 are important for the binding of PEA-15 to ERK2 (Figure 2C) (*22*). The large magnitude of the cysteine protection (110-fold) seen for the ERK2-*CT* L232C upon PEA-15 binding (Table 2 and Figures 5−7), lends further support to this mode of binding as the protein environment of Leu-232 must clearly be altered upon PEA-15 binding to induce the protection. However, a conformational change in the region of residue 232 cannot be discounted in this case as this region of ERK2 is known to exhibit significant flexibility (*44*). Natalie Ahn's laboratory analyzed the binding of the F-site peptide *N*-AKLSFQFPS-*C* derived from Elk-1 using HX-MS to first show that the F-recruitment site (FRS) lies near to the P1 site, the PEA-15 binding site (Figure 2A,C) (*44*). Mutagenesis and computer modeling studies suggested a binding mode for the peptide that is shown in Figure 2C (*44*). From this figure the close proximity of the P1 site and the FRS is apparent. We are interested in identifying ERK2 inhibitors that bind the FRS and recently showed that the transcription factor Ets-1 is displaced from ERK2 by the F-site peptide *N*-AKLSFQFPS-*C*, which binds with a dissociation constant of 65 μM (*37*).

To test if the F-site peptide could displace PEA-15 from ERK2, a competition assay was performed where 100 nM PEA-15* was competed against 0−171 μM of the F-site peptide, for the binding to 625 nM of activated ERK2. The F-site peptide does not bind unactivated ERK2 (*37*) and therefore is not expected to displace PEA-15* from unactivated ERK2, as indeed was shown to be the case (data not shown). Surprisingly, however, the F-site peptide also failed to displace PEA-15* from activated ERK2 (Figure 4). Under these conditions approximately 55% of the PEA-15* is

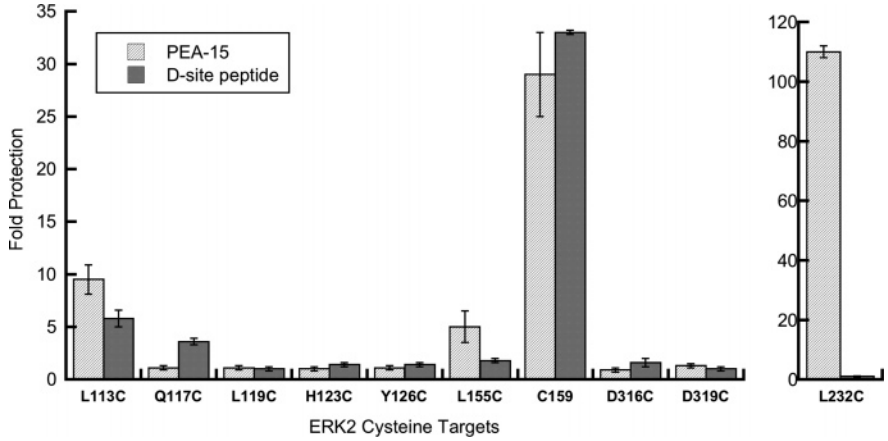

FIGURE 7: Fold protection of ERK2-*CTs* by PEA-15 and the D-site peptide.

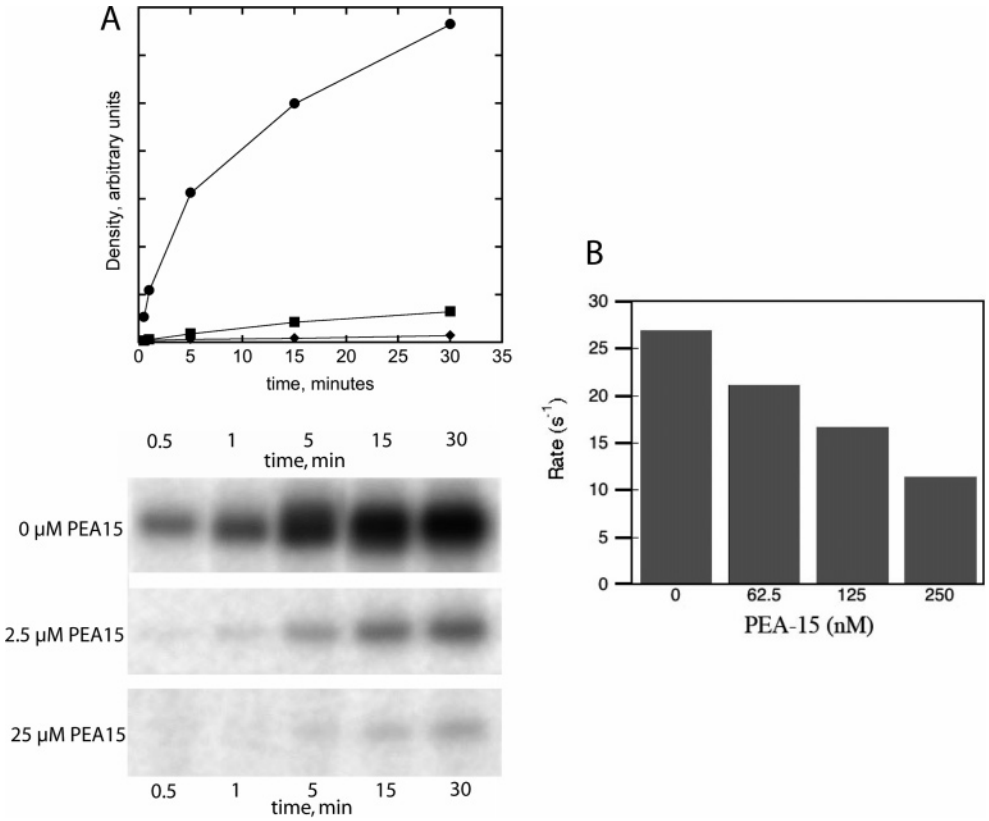

FIGURE 8: Inhibition of ERK2 by PEA-15. A. Inhibition of Elk-1 phosphorylation by PEA-15. Inhibition assays contained 2 nM activated ERK2, 4 μM GST-Elk1, and 300 μM [γ-^{32}P]-ATP at varied concentrations of PEA-15 (0, 2.5, and 25 μM). Aliquots were taken at various time points and run on a 10% SDS−PAGE gel (bottom). The gel was exposed to phosphor screens, and the amount of radiolabeled phosphorylated Elk-1 was determined using the program ImageQuant. The plot displays the relative amount of radioactivity associated with Elk-1 at the time point indicated for each concentration of PEA-15 (0, ●; 2.5, ■; and 25 μM, ◆). B. Inhibition of EtsΔ138 phosphorylation by PEA-15. Inhibition assays contained 2 nM activated ERK2, 2 mM [γ-^{32}P]-ATP, and 100 μM EtsΔ138 at varied concentrations of PEA-15 (0−250 nM). Initial rates were determined by fitting plots of product against time to the equation of a line.

complexed to activated ERK2 in the absence of a competitor[3] and full dissociation of the complex is calculated to furnish a fall in the solution anisotropy value, r, from $r = 0.26$ to $r = 0.20$. Despite the concentration of the F-site peptide exceeding the dissociation constant for the ERK2·peptide complex by 2.6-fold, only a minor decrease in the anisotropy is observed. Under similar conditions, the dissociation of the ERK2·EtsΔ138 complex was easily observed (*37*). This suggests that, although PEA-15 binds the P1 site, it does not bind the FRS in a manner that displaces the peptide, suggesting that inhibitors based on the F-site peptide may selectively inhibit the formation of some ERK2−substrate complexes, but not the ERK2−PEA15 complex. It is possibile that the peptide adopts a slightly different orientation in the complex to that shown in Figure 2C.

PEA-15 Inhibits ERK1/2

Given the proposed mode of binding, PEA-15 is expected to inhibit the interactions of many regulators and substrates of ERK1/2 that bind the DRS. However, it has been

[3] Determined from quadratic equation (EP) $K_d = (a_0 - EP)(e_0 - EP)$ where EP is the concentration of the complex and e_0 and a_0 are the concentrations of ERK2 and PEA-15, respectively.

suggested that PEA-15 does not prevent ERK2 from phosphorylating substrates (*21*). We decided to re-examine this proposal, because several studies have shown that D-site peptides strongly inhibit the ability of MAPKs to recruit and phosphorylate their cognate substrates (*45*−*47*). We reasoned that if PEA-15 uses a D-site for binding, it should inhibit the phosphorylation of substrates containing D-sites.

To test this hypothesis we chose two substrates known to bind the DRS of ERK2: Elk-1 (*48*) and Ets-1 (*29*). Inhibition assays were performed by adding increasing amounts of PEA-15 to Elk-1 and ERK2 in the presence of [γ-^{32}P]-ATP (Figure 8A). In the absence of PEA-15, the detection of phosphorylated Elk-1 occurred as early as 30 s and the amount of phosphorylated Elk-1 continued to increase during the course of the reaction. In comparison, when 2.5 μM PEA-15 was present phosphorylated Elk-1 was not significantly detected until 5 min and when 25 μM PEA-15 was added it took 15−30 min to appear. As the reactions continued, increasing amounts of phosphorylated Elk-1 were detected, but the amount was drastically less than that seen in the absence of PEA-15. These results clearly demonstrate the ability of PEA-15 to inhibit the ERK2-catalyzed phosphorylation of Elk-1 and can be used to estimate an IC_{50} value of less than 1 μM, which is consistent with the binding affinities that were determined (Table 1). To examine the ability of PEA-15 to inhibition the phosphorylation of EtsΔ138, increasing amounts of PEA-15 were added to EtsΔ138 and ERK2 in the presence of [γ-^{32}P]-ATP. As shown in Figure 8B, the rate of the reaction decreased with increasing concentrations of PEA-15, proving that PEA-15 also inhibits the phosphorylation of EtsΔ138. Thus, contrary to a previous report, where low concentrations of PEA-15 were used (*21*), PEA-15 is shown to be a potent inhibitor of ERK2.

It is interesting that the overexpression of PEA-15 leads to more robust activation of ERK2, despite the expected ability of PEA-15 to compete with MKK1 for binding to it (*9*). In light of the new evidence that PEA-15 inhibits ERK2, one possible explanation for this observation is that PEA-15 prevents the phosphorylation of several upstream components of the signaling pathway, such as SOS (*49*), Raf (*50*), and MEK (*51*), which may result in a greater activation of pools of MEK and ERK1/2. However, the intriguing ability of overexpressed PEA-15 to inhibit the phosphorylation of Elk-1 in the nucleus, but not the phosphorylation of the cytoplasmic proteins stathmin and p90RSK, suggests that this might not be the reason. Although it is possible that different signaling thresholds operate in the nucleus compared to the cytoplasm, another possibility is that PEA-15 only has access to cytoplasmic pools of ERK2 that are not protected by protein complexes. Such sequestering of free ERK2 could potentially be a mechanism by which PEA-15 contributes to the specificity of ERK2 signaling. Clearly, the development of cell permeable ERK1/2-selective inhibitors would greatly help in furthering our understanding of the cellular processes that regulate ERK2 and in evaluating the potential of ERK1/2 as a drug target.

ACKNOWLEDGMENT

We are indebted to Dr. Melanie Cobb (UT Southwestern Medical Center) and Dr. Natalie G. Ahn (University of Colorado at Boulder) for generously providing us with DNA encoding His_6-ERK2 and His_6-MKK1G7B, respectively.

SUPPORTING INFORMATION AVAILABLE

Experimental procedures and ESI mass spectra. This material is available free of charge via the Internet at http://pubs.acs.org.

REFERENCES

1. Lewis, T. S., Shapiro, P. S., and Ahn, N. G. (1998) Signal transduction through MAP kinase cascades, *Adv. Cancer Res. 74*, 49−139.
2. Seger, R., and Krebs, E. G. (1995) The MAPK signaling cascade, *FASEB J. 9*, 726−735.
3. Chen, Z., Gibson, T. B., Robinson, F., Silvestro, L., Pearson, G., Xu, B., Wright, A., Vanderbilt, C., and Cobb, M. H. (2001) MAP kinases, *Chem. Rev. 101*, 2449−2476.
4. Kumar, S., Boehm, J., and Lee, J. C. (2003) p38 MAP kinases: key signalling molecules as therapeutic targets for inflammatory diseases, *Nat. Rev. Drug Discovery 2*, 717−726.
5. Davis, R. J. (2000) Signal transduction by the JNK group of MAP kinases, *Cell 103*, 239−252.
6. Lenormand, P., Brondello, J. M., Brunet, A., and Pouyssegur, J. (1998) Growth factor-induced p42/p44 MAPK nuclear translocation and retention requires both MAPK activation and neosynthesis of nuclear anchoring proteins, *J. Cell Biol. 142*, 625−633.
7. Traverse, S., Gomez, N., Paterson, H., Marshall, C., and Cohen, P. (1992) Sustained activation of the mitogen-activated protein (MAP) kinase cascade may be required for differentiation of PC12 cells. Comparison of the effects of nerve growth factor and epidermal growth factor, *Biochem. J. 288* (Part 2), 351−355.
8. Horgan, A. M., and Stork, P. J. (2003) Examining the mechanism of Erk nuclear translocation using green fluorescent protein, *Exp. Cell Res. 285*, 208−220.
9. Whitehurst, A. W., Robinson, F. L., Moore, M. S., and Cobb, M. H. (2004) The death effector domain protein PEA-15 prevents nuclear entry of ERK2 by inhibiting required interactions, *J. Biol. Chem. 279*, 12840−12847.
10. Burack, W. R., and Shaw, A. S. (2005) Live Cell Imaging of ERK and MEK: simple binding equilibrium explains the regulated nucleocytoplasmic distribution of ERK, *J. Biol. Chem. 280*, 3832−3837.
11. Ranganathan, A., Yazicioglu, M. N., and Cobb, M. H. (2006) The nuclear localization of ERK2 occurs by mechanisms both independent of and dependent on energy, *J. Biol. Chem. 281*, 15645−15652.
12. Rubinfeld, H., Hanoch, T., and Seger, R. (1999) Identification of a cytoplasmic-retention sequence in ERK2, *J. Biol. Chem. 274*, 30349−30352.
13. Tohgo, A., Pierce, K. L., Choy, E. W., Lefkowitz, R. J., and Luttrell, L. M. (2002) beta-Arrestin scaffolding of the ERK cascade enhances cytosolic ERK activity but inhibits ERK-mediated transcription following angiotensin AT1a receptor stimulation, *J. Biol. Chem. 277*, 9429−9436.
14. Zhang, S., Fukushi, M., Hashimoto, S., Gao, C., Huang, L., Fukuyo, Y., Nakajima, T., Amagasa, T., Enomoto, S., Koike, K., Miura, O., Yamamoto, N., and Tsuchida, N. (2002) A new ERK2 binding protein, Naf1, attenuates the EGF/ERK2 nuclear signaling, *Biochem. Biophys. Res. Commun. 297*, 17−23.
15. Torii, S., Kusakabe, M., Yamamoto, T., Maekawa, M., and Nishida, E. (2004) Sef is a spatial regulator for Ras/MAP kinase signaling, *Dev. Cell 7*, 33−44.
16. Zuniga, A., Torres, J., Ubeda, J., and Pulido, R. (1999) Interaction of mitogen-activated protein kinases with the kinase interaction motif of the tyrosine phosphatase PTP-SL provides substrate specificity and retains ERK2 in the cytoplasm, *J. Biol. Chem. 274*, 21900−21907.
17. Callaway, K., Rainey, M. A., and Dalby, K. N. (2005) Quantifying ERK2-protein interactions by fluorescence anisotropy: PEA-15 inhibits ERK2 by blocking the binding of DEJL domains, *Biochim. Biophys. Acta 1754*, 316−323.
18. Chen, F., Hancock, C. N., Macias, A. T., Joh, J., Still, K., Zhong, S., Mackerell, A. D., Jr., and Shapiro, P. (2006) Characterization of ATP-independent ERK inhibitors identified through in silico

analysis of the active ERK2 structure, *Bioorg. Med. Chem.* Lett *16*, 6281−6287.
19. Hancock, C. N., Macias, A., Lee, E. K., Yu, S. Y., Mackerell, A. D., Jr., and Shapiro, P. (2005) Identification of novel extracellular signal-regulated kinase docking domain inhibitors, *J. Med. Chem. 48*, 4586−4595.
20. Araujo, H., Danziger, N., Cordier, J., Glowinski, J., and Chneiweiss, H. (1993) Characterization of PEA-15, a major substrate for protein kinase C in astrocytes, *J. Biol. Chem. 268*, 5911−5920.
21. Formstecher, E., Ramos, J. W., Fauquet, M., Calderwood, D. A., Hsieh, J. C., Canton, B., Nguyen, X. T., Barnier, J. V., Camonis, J., Ginsberg, M. H., and Chneiweiss, H. (2001) PEA-15 mediates cytoplasmic sequestration of ERK MAP kinase, *Dev. Cell 1*, 239−250.
22. Hill, J. M., Vaidyanathan, H., Ramos, J. W., Ginsberg, M. H., and Werner, M. H. (2002) Recognition of ERK MAP kinase by PEA-15 reveals a common docking site within the death domain and death effector domain, *EMBO J. 21*, 6494−6504.
23. Gill, S. C., and von Hippel, P. H. (1989) Calculation of protein extinction coefficients from amino acid sequence data, *Anal. Biochem. 182*, 319−326.
24. Jacobs, D., Glossip, D., Xing, H., Muslin, A. J., and Kornfeld, K. (1999) Multiple docking sites on substrate proteins form a modular system that mediates recognition by ERK MAP kinase, *Genes Dev. 13*, 163−175.
25. Yang, S. H., Galanis, A., and Sharrocks, A. D. (1999) Targeting of p38 mitogen-activated protein kinases to MEF2 transcription factors, *Mol. Cell. Biol. 19*, 4028−4038.
26. Khokhlatchev, A., Xu, S., English, J., Wu, P., Schaefer, E., and Cobb, M. H. (1997) Reconstitution of mitogen-activated protein kinase phosphorylation cascades in bacteria. Efficient synthesis of active protein kinases, *J. Biol. Chem. 272*, 11057−11062.
27. Sechi, S., and Chait, B. T. (1998) Modification of cysteine residues by alkylation. A tool in peptide mapping and protein identification, *Anal. Chem. 70*, 5150−5158.
28. Walsh, D. A., Ashby, C. D., Gonzalez, C., Calkins, D., and Fischer, E. H. (1971) Krebs EG: Purification and characterization of a protein inhibitor of adenosine 3′,5′-monophosphate-dependent protein kinases, *J. Biol. Chem. 246*, 1977−1985.
29. Abramczyk, O., Rainey, M. A., Barnes, R., Martin, L., and Dalby, K. N. (2007) Expanding the Repertoire of an ERK2 Recruitment Site: Cysteine Footprinting Identifies the D-Recruitment Site as a Mediator of Ets-1 Binding, *Biochemistry 46*, 9174−9186.
30. Condorelli, G., Vigliotta, G., Iavarone, C., Caruso, M., Tocchetti, C. G., Andreozzi, F., Cafieri, A., Tecce, M. F., Formisano, P., Beguinot, L., and Beguinot, F. (1998) PED/PEA-15 gene controls glucose transport and is overexpressed in type 2 diabetes mellitus, *EMBO J. 17*, 3858−3866.
31. Ramos, J. W., Kojima, T. K., Hughes, P. E., Fenczik, C. A., and Ginsberg, M. H. (1998) The death effector domain of PEA-15 is involved in its regulation of integrin activation, *J. Biol. Chem. 273*, 33897−33900.
32. Gaumont-Leclerc, M. F., Mukhopadhyay, U. K., Goumard, S., and Ferbeyre, G. (2004) PEA-15 is inhibited by adenovirus E1A and plays a role in ERK nuclear export and Ras-induced senescence, *J. Biol. Chem. 279*, 46802−46809.
33. Kitsberg, D., Formstecher, E., Fauquet, M., Kubes, M., Cordier, J., Canton, B., Pan, G., Rolli, M., Glowinski, J., and Chneiweiss, H. (1999) Knock-out of the neural death effector domain protein PEA-15 demonstrates that its expression protects astrocytes from TNFalpha-induced apoptosis, *J. Neurosci. 19*, 8244−8251.
34. Danziger, N., Yokoyama, M., Jay, T., Cordier, J., Glowinski, J., and Chneiweiss, H. (1995) Cellular expression, developmental regulation, and phylogenic conservation of PEA-15, the astrocytic major phosphoprotein and protein kinase C substrate, *J. Neurochem. 64*, 1016−1025.
35. Renganathan, H., Vaidyanathan, H., Knapinska, A., and Ramos, J. W. (2005) Phosphorylation of PEA-15 switches its binding specificity from ERK/MAPK to FADD, *Biochem. J. 390*, 729−735.
36. Krueger, J., Chou, F. L., Glading, A., Schaefer, E., and Ginsberg, M. H. (2005) Phosphorylation of phosphoprotein enriched in astrocytes (PEA-15) regulates extracellular signal-regulated kinase-dependent transcription and cell proliferation, *Mol. Biol. Cell 16*, 3552−3561.
37. Callaway, K. A., Rainey, M. A., Riggs, A. F., Abramczyk, O., and Dalby, K. N. (2006) Properties and regulation of a transiently assembled ERK2.Ets-1 signaling complex, *Biochemistry 45*, 13719−13733.
38. Chou, F. L., Hill, J. M., Hsieh, J. C., Pouyssegur, J., Brunet, A., Glading, A., Uberall, F., Ramos, J. W., Werner, M. H., and Ginsberg, M. H. (2003) PEA-15 binding to ERK1/2 MAPKs is required for its modulation of integrin activation, *J. Biol. Chem. 278*, 52587−52597.
39. Sharrocks, A. D., Yang, S. H., and Galanis, A. (2000) Docking domains and substrate-specificity determination for MAP kinases, *Trends Biochem. Sci. 25*, 448−453.
40. Holland, P. M., and Cooper, J. A. (1999) Protein modification: docking sites for kinases, *Curr. Biol. 9*, R329−331.
41. Canagarajah, B. J., Khokhlatchev, A., Cobb, M. H., and Goldsmith, E. J. (1997) Activation mechanism of the MAP kinase ERK2 by dual phosphorylation, *Cell 90*, 859−869.
42. Liu, S., Sun, J. P., Zhou, B., and Zhang, Z. Y. (2006) Structural basis of docking interactions between ERK2 and MAP kinase phosphatase 3, *Proc. Natl. Acad. Sci. U.S.A. 103*, 5326−5331.
43. Zhou, T., Sun, L., Humphreys, J., and Goldsmith, E. J. (2006) Docking interactions induce exposure of activation loop in the MAP kinase ERK2, *Structure 14*, 1011−1019.
44. Lee, T., Hoofnagle, A. N., Kabuyama, Y., Stroud, J., Min, X., Goldsmith, E. J., Chen, L., Resing, K. A., and Ahn, N. G. (2004) Docking motif interactions in MAP kinases revealed by hydrogen exchange mass spectrometry, *Mol. Cell 14*, 43−55.
45. Ho, D. T., Bardwell, A. J., Abdollahi, M., and Bardwell, L. (2003) A docking site in MKK4 mediates high affinity binding to JNK MAPKs and competes with similar docking sites in JNK substrates, *J. Biol. Chem. 278*, 32662−32672.
46. Bardwell, A. J., Abdollahi, M., and Bardwell, L. (2003) Docking sites on mitogen-activated protein kinase (MAPK) kinases, MAPK phosphatases and the Elk-1 transcription factor compete for MAPK binding and are crucial for enzymic activity, *Biochem. J. 370*, 1077−1085.
47. Yang, S. H., Whitmarsh, A. J., Davis, R. J., and Sharrocks, A. D. (1998) Differential targeting of MAP kinases to the ETS-domain transcription factor Elk-1, *EMBO J. 17*, 1740−1749.
48. Yang, S. H., Yates, P. R., Whitmarsh, A. J., Davis, R. J., and Sharrocks, A. D. (1998) The Elk-1 ETS-domain transcription factor contains a mitogen-activated protein kinase targeting motif, *Mol. Cell. Biol. 18*, 710−720.
49. Douville, E., and Downward, J. (1997) EGF induced SOS phosphorylation in PC12 cells involves P90 RSK-2, *Oncogene 15*, 373−383.
50. Dougherty, M. K., Muller, J., Ritt, D. A., Zhou, M., Zhou, X. Z., Copeland, T. D., Conrads, T. P., Veenstra, T. D., Lu, K. P., and Morrison, D. K. (2005) Regulation of Raf-1 by direct feedback phosphorylation, *Mol. Cell 17*, 215−224.
51. Brunet, A., Pages, G., and Pouyssegur, J. (1994) Growth factor-stimulated MAP kinase induces rapid retrophosphorylation and inhibition of MAP kinase kinase (MEK1), *FEBS Lett. 346*, 299−303.

BI700206U